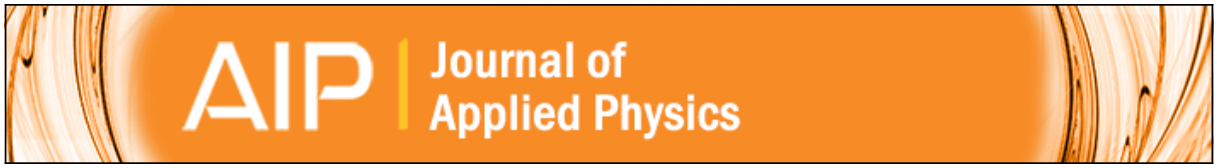

Compositional and valent state inhomogeneities and ordering of oxygen vacancies in terbium-doped ceria

Fei Ye, Toshiyuki Mori, Ding Rong Ou, Jin Zou, Graeme Auchterlonie, and John Drennan

Citation: Journal of Applied Physics **101**, 113528 (2007); doi: 10.1063/1.2738409

View online: http://dx.doi.org/10.1063/1.2738409

View Table of Contents: http://scitation.aip.org/content/aip/journal/jap/101/11?ver=pdfcov

Published by the AIP Publishing

Compositional and valent state inhomogeneities and ordering of oxygen vacancies in terbium-doped ceria

Fei Ye,[a] Toshiyuki Mori, and Ding Rong Ou
Fuel Cell Materials Center, National Institute for Materials Science, 1-1 Namiki, Tsukuba, Ibaraki 305-0044, Japan

Jin Zou
School of Engineering and Centre for Microscopy and Microanalysis, The University of Queensland, St. Lucia, Brisbane, QLD 4072, Australia

Graeme Auchterlonie and John Drennan
Centre for Microscopy and Microanalysis, The University of Queensland, St. Lucia, Brisbane, QLD 4072, Australia

(Received 7 February 2007; accepted 4 March 2007; published online 12 June 2007)

Intragranular distributions of composition and valent state in sintered Tb-doped ceria have been systematically investigated. Through detailed studies of electron energy loss spectroscopy and energy filtering transmission electron microscopy, both compositional and valent state inhomogeneities of Ce and Tb were confirmed, which are related to the existence of nanosized domains in Tb-doped ceria. Compared with their matrix, the domains have higher Tb concentration and Ce and Tb cations in the domains tend to be trivalent. Furthermore, ordering of oxygen vacancies in the domains, which increases with increasing doping concentration, has been determined by EELS. © *2007 American Institute of Physics*. [DOI: 10.1063/1.2738409]

I. INTRODUCTION

Ceria-based oxides have been widely used as three-way catalysts,[1,2] oxygen permeation membranes,[3] oxygen gas sensors,[4] as well as electrolytes and electrodes of solid oxide fuel cells (SOFCs).[5] Among these doped ceria materials, Tb-doped ceria presents electrical properties of mixed conductors (electronic and ionic), which can be of interest for their potential applications as electrodes for intermediate temperature SOFCs and for oxygen membranes.[6] Furthermore, Tb-doped ceria continues to attract attention because it has been shown to be advantageous for the performance of three-way catalysts.[7–9] In contrast to other widely studied rare-earth-doped ceria materials, in which the dopant cations are trivalent (such as Y^{3+}, Gd^{3+}, and Sm^{3+}) and Ce is dominantly tetravalent, Tb and Ce in Tb-doped ceria have shown mixed valence (trivalent and tetravalent),[6,10,11] which can, in turn, contribute to the mixed conduction and the catalytic property. For this reason, it is technologically important to understand their valence behaviors in Tb-doped ceria.

Recently, nanosized domains in various ceria-based oxides [such as La^{3+}-,[12] Sm^{3+}-,[13,14] Dy^{3+}-,[15] and Y^{3+}[16,17] -doped ceria] have been observed using high resolution transmission electron microscopy (HRTEM). A study of energy filtering transmission electron microscopy (EFTEM) in Y-doped ceria indicated that the dopant cations could segregate in the domains.[18] Consequently, oxygen vacancies may be attracted by the domains.[17,18] Although the crystal structure of the domains remains unclear, it has been anticipated that the oxygen vacancies in the domains are partly ordered.[19] Because the mobility of oxygen vacancies can be decreased by ordering, the domains would have a negative impact on the ionic conduction of doped ceria. In the case of Tb-doped ceria, domains were also observed,[11] but their detailed compositional and valent state characteristics remain unclear. It is expected that the formation of the domains in Tb-doped ceria should be related to a compositional inhomogeneity, i.e., the segregation of dopant cations in the domains. Furthermore, since both Ce and Tb have mixed valence in this material, the valent state of the cations may also influence the formation of the domains and thereby the electrical properties of Tb-doped ceria. For these reasons, both the compositional and valent state characteristics in Tb-doped ceria deserve a detailed investigation.

In this study, the distributions of composition and valent state in $Ce_{1-x}Tb_xO_{2-\delta}$ $(0 \leq x \leq 0.50)$ sintered samples and the ordering of oxygen vacancies in the domains are studied systematically by using EFTEM and electron energy loss spectroscopy (EELS). The relationship between the compositional and valent state distributions and the formation of the domains is discussed.

II. EXPERIMENTAL

Four highly dense $Ce_{1-x}Tb_xO_{2-\delta}$ (x=0, 0.1, 0.25, and 0.50) sintered samples were prepared from nanopowders synthesized via the ammonium carbonate coprecipitation method. A detailed description of the process of powder synthesis can be found in Ref. 20. The powders were isostatically pressed under 200 MPa pressure to form compacts which were heated to 1400 °C at a rate of 5 °C/min in air. After holding for 6 h, the samples were cooled to room temperature at a rate of 5 °C/min.

In the preparation of transmission electron microscopy (TEM) specimens, small disks with a diameter of 3 mm were

[a]Electronic mail: fei.ye@nims.go.jp

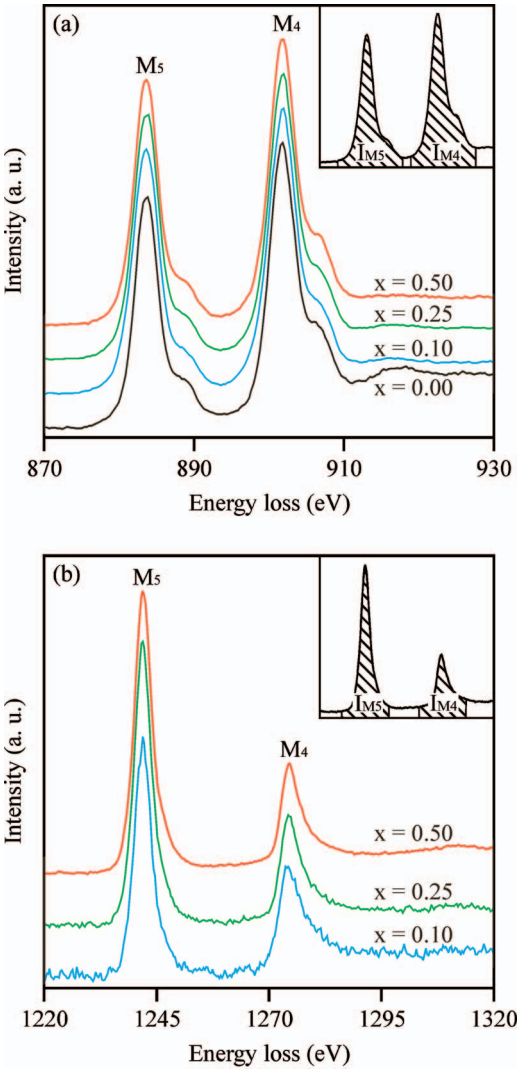

FIG. 1. (Color) (a) Ce and (b) Tb $M_{4,5}$ edges of $Ce_{1-x}Tb_xO_{2-\delta}$ samples. The insets illustrate the calculation of integral intensities of M_4 and M_5 peaks I_{M_4} and I_{M_5}.

cut with an ultrasonic cutter from the sintered samples. The disks were thinned to a thickness of ~70 μm by mechanical grinding and dimpled to a central thickness of ~30 μm, followed by ion beam thinning. TEM investigations were performed using a JEOL JEM 2000EX TEM. EFTEM and EELS were conducted on a FEI Tecnai G^2 F30 TEM equipped with a Gatan imaging filtering system and operated at an accelerating voltage of 300 kV. The EELS spectra were acquired using a collection aperture size of 2 mm, an acquisition time of about 2–3 s and an energy dispersion of 0.3 eV per channel. After calibration of the spectra, the background was removed using a power-law technique.[21]

III. RESULTS

A. Compositional and valent state characterization

The mixed valence of Ce and Tb in the samples was examined by using EELS. Figure 1 shows the Ce and Tb $M_{4,5}$ edges of all sintered samples. These spectra were taken from large areas (about 100 nm) in the samples, so they should correspond to the average compositions of the samples. The two peaks (labeled M_4 and M_5) reflect the transitions of $3d$ core electrons to unoccupied states of p- and f-like symmetry. Their relative intensities could be used to determine the occupancy of the $4f$ orbital and, hence, the valence of lanthanide cations.[22–24] Practically, the intensity increase of M_5 peak indicates an increase in trivalent cation concentration of lanthanides.[22–26] In this study, to qualitatively estimate the trivalent cation concentration in all sintered samples, the comparison of relative intensities of M_4 and M_5 peaks for a given sample and a given element (Ce or Tb in this case) was carried out by comparing the integral intensities of the corresponding M_4 and M_5 peaks (i.e., I_{M_4} and I_{M_5}). Each integral intensity was calculated using energy windows with a width of 16 eV for Ce and 20 eV for Tb (as illustrated by the insets in Fig. 1), respectively. The I_{M_5}/I_{M_4} values were then calculated and listed in Table I. As can be seen from Table I, the I_{M_5}/I_{M_4} values for Ce in all Tb-doped ceria samples are almost the same, but slightly larger than that of pure ceria, indicating that all Tb-doped ceria samples contain a small amount of Ce^{3+} cations. On the other hands, the I_{M_5}/I_{M_4} value for Tb increases with increasing doping concentration, indicating that the heavily doped ceria samples have higher content of Tb^{3+} cations.

TABLE I. I_{M_5}/I_{M_4} values of Ce and Tb $M_{4,5}$ edges and I_B/I_C values of the oxygen K edge of $Ce_{1-x}Tb_xO_{2-\delta}$ samples

Tb concentration x	I_{M_5}/I_{M_4} Ce	I_{M_5}/I_{M_4} Tb	I_B/I_C
0.00	0.66		0.64
0.10	0.72	1.31	0.77
0.25	0.72	1.86	0.80
0.50	0.72	1.83	0.90

Next, the intragranular distributions of composition and valent state of cations were studied. To observe the compositional distribution in the sintered samples, EFTEM was used to perform the elemental mapping. Because of the high intensities of Ce and Tb $N_{4,5}$ edges, EFTEM elemental maps of Ce and Tb were obtained by using $N_{4,5}$ edges with an energy window of 10 eV opened on the edges. The three-window power-law technique[21] was used to subtract the background. If the sample is uniformly thin and deviates away from the strong Bragg reflection conditions, the brightness of the map is proportional to the composition of the mapping element.[21] Figure 2 shows Ce and Tb maps of $Ce_{1-x}Tb_xO_{2-\delta}$ samples with x=0.10 and 0.50. We chose uniformly thin TEM foil to perform EFTEM, so that the uneven contrast shown in Fig. 2 suggests that the compositional distribution of both Ce and Tb is inhomogeneous in the two samples. Dark regions in the Ce map with a size between 10–20 nm (enclosed by dashed lines) are bright in the Tb map, indicating that these regions have a higher Tb concentration than their surrounding matrix. The density of such compositional inhomogeneity is higher in the sample with higher Tb concentration. In our previous study,[11] nanosized domains were observed by HRTEM. Because the size and distribution of these regions in Fig. 2 are similar to the domains, we believe that these regions are the domains and

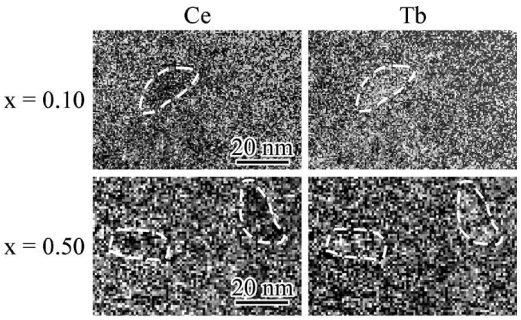

FIG. 2. Elemental maps of Ce and Tb of $Ce_{1-x}Tb_xO_{2-\delta}$ samples with x =0.10 and 0.50.

there is a compositional inhomogeneity between the domains and the matrix. The compositions of the domains and the matrix were further confirmed by EELS as the electron beam was focused on the domains and the matrix, respectively. As given in Table II, in the sample with x=0.50, the Tb concentration of a domain was measured to be 52 at. %, while the Tb concentration of its surrounding matrix decreased to 43 at. %. However, because the domains are well dispersed in the matrix, it is difficult to totally separate the domain and the matrix during the EELS analysis. Therefore, the actual compositional difference between domains and the matrix can be larger than the measured result.

Furthermore, it was found that the compositional inhomogeneity is always accompanied by an uneven distribution of the valent states of Ce and Tb. Figure 3 shows EELS spectra of Ce and Tb $M_{4,5}$ edges of a domain and its surrounding matrix in the sample with x=0.50, which were normalized with respect to the intensity of the peak M_4. The I_{M_5}/I_{M_4} values were also calculated and given in Table II. It is clearly shown that the I_{M_5}/I_{M_4} values of both Ce and Tb in the domains are higher than those of the matrix, indicating that both Ce^{3+} and Tb^{3+} cations segregate in the domains.

B. Ordering of oxygen vacancies in the domains

Figure 4 shows selected area electron diffraction (SAED) patterns from two samples with x=0.10 and 0.50, taken from different zone axes [110] and [112]. Strong reflections of the typical fluorite structure can be seen in all SAED patterns, indicating that all samples contain mainly fluorite structure. However, as the Tb concentration increases, weak diffuse scattering and extra reflections as indicated by arrows can be clearly seen. As mentioned previously, the density of the domains increases with increasing doping concentration. Taking these two facts into account, it

TABLE II. Compositions, I_{M_5}/I_{M_4} values of Ce and Tb $M_{4,5}$ edges, and I_B/I_C values of the oxygen K edge of a domain and its surrounding matrix in the $Ce_{0.5}Tb_{0.5}O_{2-\delta}$ sample

	Composition (atomic ratio)		I_{M_5}/I_{M_4}		
	Ce	Tb	Ce	Tb	I_B/I_C
Domain	0.48	0.52	0.83	1.75	1.03
Matrix	0.57	0.43	0.70	1.41	0.81

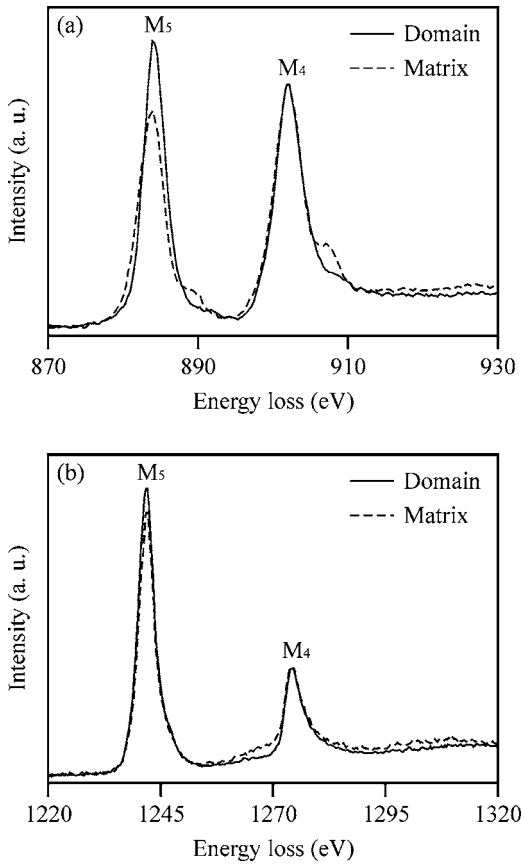

FIG. 3. (a) Ce and (b) Tb $M_{4,5}$ edges of a domain and its surrounding matrix in the $Ce_{0.5}Tb_{0.5}O_{2-\delta}$ sample.

can be suggested that the diffuse scattering and extra reflections are related to the domains and that the domains have an ordered structure that is different than the fluorite-structured matrix. Since the aforementioned results have demonstrated that trivalent cations tend to segregate in the domains, the oxygen vacancies may be trapped by the domains due to the

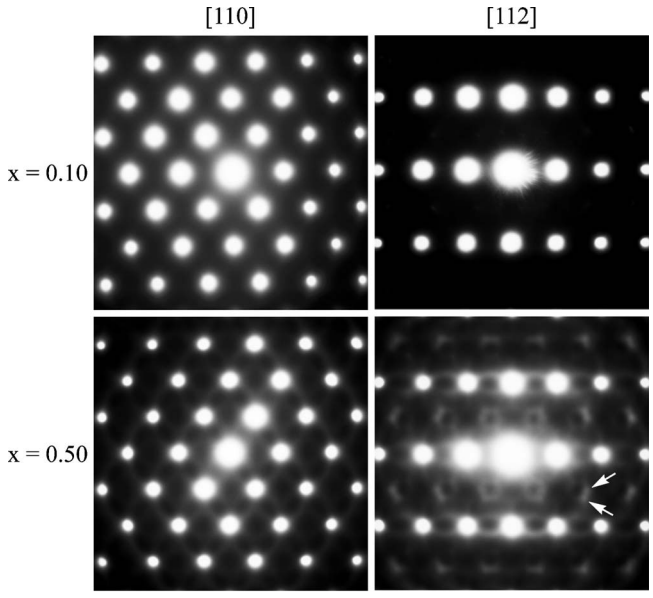

FIG. 4. [110] and [112] SAED patterns of $Ce_{1-x}Tb_xO_{2-\delta}$ samples with x =0.10 and 0.50.

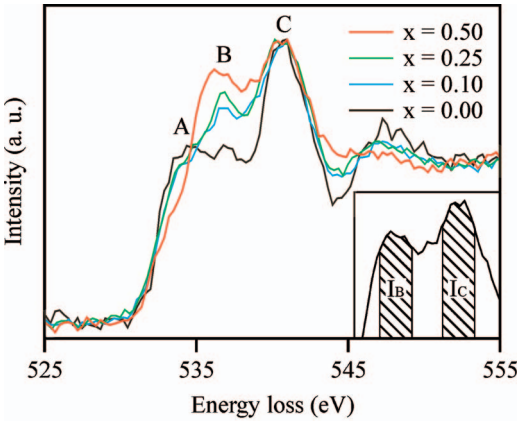

FIG. 5. (Color) Oxygen K edges of $Ce_{1-x}Tb_xO_{2-\delta}$ samples. The inset illustrates the calculation of integral intensities of peaks B and C, I_B and I_C.

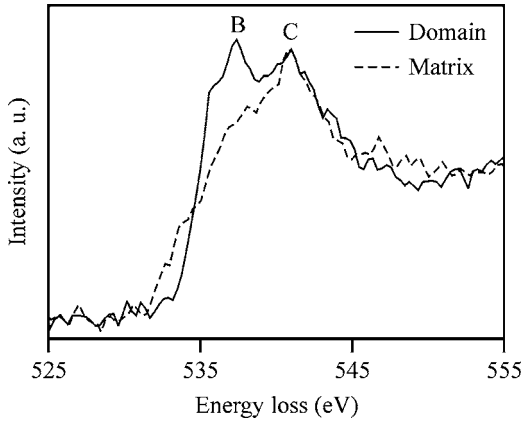

FIG. 6. Oxygen K edges of a domain and its surrounding matrix in the $Ce_{0.5}Tb_{0.5}O_{2-\delta}$ sample.

requirement of electrical neutrality. This can be supported by theoretical calculations, which showed that the neutral clusters are more thermodynamically favorable than the clusters containing only dopant cations or oxygen vacancies.[27,28] As a consequence, the domains would have a higher concentration of oxygen vacancies and, in turn, the ordered structure of the domains possibly involves an ordering of these oxygen vacancies.

To confirm the hypothesis of ordering of oxygen vacancies, EELS investigation was carried out, since previous studies have demonstrated that the ordering of oxygen vacancies in nonstoichiometric oxides can be determined from the near edge fine structure of the oxygen K edge.[19,29] Figure 5 shows oxygen K edges for all samples taken from large areas, so that the results should correspond to the average results. Three peaks, marked by A, B, and C, can be seen in Fig. 5. Peak A results from the hybridization between oxygen and Ce^{4+} cations,[30,31] which is obvious in pure ceria and becomes weak in doped ceria because of the decrease of the Ce concentration in doped ceria. As for the case of peaks B and C, previous studies have shown that the relative intensities of the peaks can be influenced by the crystal structure[30,31] and the enhancement of peak B could be due to the ordering of oxygen vacancies in nonstoichiometric oxides.[19,29] To compare the relative intensities of peaks B and C, the spectra in Fig. 5 are normalized with respect to the intensity of peak C. The integral intensities of peaks B and C, I_B and I_C, were calculated using energy windows with a width of 2 eV, as illustrated by the inset in Fig. 5. The I_B/I_C values were then calculated and listed in Table I. As shown in Fig. 5 and Table I, the I_B/I_C value increases with increasing Tb concentration, indicating the increase in the ordering of oxygen vacancies.

Furthermore, the EELS analysis reveals that this ordering of oxygen vacancies is mainly related to the domains. Figure 6 shows the oxygen K edges of a domain and its surrounding matrix in the sample with $x=0.50$, whose values of I_B/I_C are calculated and given in Table II. As can be noted from Fig. 6 and Table II, the intensity of the peak B of the domains is much higher than that of the matrix, indicating the considerable ordering of oxygen vacancies in the domains.

IV. DISCUSSION

The above results have shown that the compositional and valent state inhomogeneities are related to the existence of domains. The fact that these domains have higher dopant concentration than the matrix is consistent with the previous observation in Y-doped ceria.[18] Based on the EFTEM study,[18] it had been suggested that the domain formation in Y-doped ceria results from the segregation of dopant cations. In addition to the dopant segregation, the results presented in this study reveal that the domain formation in Tb-doped ceria is not only related to the segregation of the dopant, but also to the segregation of trivalent cations. Both Tb^{3+} and Ce^{3+} cations segregate in the domains, though Ce^{3+} is not a dopant cation and the concentration of Ce in the domains is lower than that in the matrix. This phenomenon has not been seen in Y-doped ceria, in which Y is solely trivalent and Ce is dominantly tetravalent.

We anticipate that one possible reason for the segregation of trivalent cations in the domains is that the oxygen coordination numbers of trivalent cations and of tetravalent cations in doped ceria with fluorite structure are different. The oxygen coordination number should be about 8 for tetravalent cations and around 7 for trivalent cations, depending upon the dopant type and concentration.[32,33] If these trivalent cations were well dispersed in the sample with the fluorite structure, they may result in a significant lattice distortion as the doping concentration is high. We suspect that as some of the trivalent cations segregate in the domains, part of the lattice distortion is localized in or around the domains so that the overall lattice distortion in the sample might decrease.

Based on all of the experimental results, we believe that domain formation in Tb-doped ceria, which involves both inhomogeneities of the composition and valent state, can be modeled as follows. During the sintering, Tb cations, especially Tb^{3+} cations, tend to segregate in some regions as the diffusion of cations takes place. Ce^{3+} cations may also tend to segregate with Tb^{3+} cations in these regions. Simultaneously, because of the requirement of electrical neutrality, the oxygen vacancies are enriched in these regions with a high concentration of trivalent cations. These segregations could lead to the formation of nanosized domains. As the doping concentration increases, the amount of trivalent cat-

ions and oxygen vacancies increases, which promotes the segregations and, in turn, the growth of domains and the increase in the ordering of oxygen vacancies.

As suggested in a previous study,[19] since the dopant cations segregate in the domains, the ordering of oxygen vacancies in the domains tends to be similar than that in the oxide of the dopant cations. In the present case, since the domains have a higher concentration of Tb, especially Tb^{3+} cations, than that of the matrix, we believe that the ordering of oxygen vacancies is similar to that in the Tb^{3+} oxide, i.e., Tb_2O_3. However, whether this ordering also involves metal atoms remains unclear.

V. CONCLUSIONS

This EELS study showed that both Ce and Tb have mixed valence in Tb-doped ceria and that more heavily doped ceria has a higher content of Tb^{3+} cations. Compositional and valent state inhomogeneities were observed which are related to the existence of nanosized domains. In the domains, Tb concentration is higher than that of the matrix and both Tb^{3+} and Ce^{3+} cations segregate in them. Accompanied by the segregation of trivalent cations, oxygen vacancies are enriched in the domains and form an ordered structure, which has been confirmed by SAED and EELS studies. As the doping concentration increases, the segregation and oxygen vacancy ordering can be promoted. It is suggested that both inhomogeneities of composition and the valent state of cations are essential driving forces for the formation of the domains.

ACKNOWLEDGMENT

The financial support of the Japan Society for the Promotion of Science (JSPS) is gratefully acknowledged.

[1] J. Kašpar, P. Fornasiero, and M. Graziani, Catal. Today **50**, 285 (1999).
[2] A. Trovarelli, *Catalysis by Ceria and Related Materials* (Imperial College Press, London, 2002).
[3] M. Stoukides, Catal. Rev. - Sci. Eng. **42**, 1 (2000).
[4] N. Izu, W. Shin, I. Matsubara, and N. Murayama, J. Electroceram. **13**, 703 (2004).
[5] B. C. H. Steele, Solid State Ionics **134**, 3 (2000).
[6] P. Shuk, M. Greenblatt, and M. Croft, Chem. Mater. **11**, 473 (1999).
[7] S. Bernal, G. Blanco, M. A. Cauqui, P. Corchado, J. M. Pintado, and J. M. Rodríguez-Izquierdo, Chem. Commun. 1545 (1997).
[8] S. Bernal, G. Blanco, M. A. Cauqui, P. Corchado, C. Larese, J. M. Pintado, and J. M. Rodríguez-Izquierdo, Catal. Today **53**, 607 (1999).
[9] A. B. Hungría, A. Martínez-Arias, M. Fernández-García, A. Iglesias-Juez, A. Guerrero-Ruiz, J. J. Calvino, J. C. Conesa, and J. Soria, Chem. Mater. **15**, 4309 (2003).
[10] X. Wang, J. C. Hanson, G. Liu, J. A. Rodriguez, A. Iglesias-Juez, and M. Fernández-García, J. Chem. Phys. **121**, 5434 (2004).
[11] F. Ye, T. Mori, D. R. Ou, J. Zou, and J. Drennan, Mater. Res. Bull. **42**, 943 (2007).
[12] T. Mori, J. Drennan, Y. Wang, J. H. Lee, J. G. Li, and T. Ikegami, J. Electrochem. Soc. **150**, A665 (2003).
[13] T. Mori, J. Drennan, J. H. Lee, J. G. Li, and T. Ikegami, Solid State Ionics **154–155**, 461 (2002).
[14] T. Mori, Y. Wang, J. Drennan, G. Auchterlonie, J. G. Li, and T. Ikegami, Solid State Ionics **175**, 641 (2004).
[15] T. Mori, T. Kobayashi, Y. Wang, J. Drennan, T. Nishimura, J. G. Li, and H. Kobayashi, J. Am. Ceram. Soc. **88**, 1981 (2005).
[16] T. Mori, J. Drennan, Y. Wang, G. Auchterlonie, J. G. Li, and A. Yago, Sci. Technol. Adv. Mater. **4**, 213 (2003).
[17] D. R. Ou, T. Mori, F. Ye, M. Takahashi, J. Zou, and J. Drennan, Acta Mater. **54**, 3737 (2006).
[18] D. R. Ou, T. Mori, F. Ye, J. Zou, G. Auchterlonie, and J. Drennan, Electrochem. Solid-State Lett. **10**, P1 (2007).
[19] D. R. Ou, T. Mori, F. Ye, T. Kobayashi, J. Zou, G. Auchterlonie, and J. Drennan, Appl. Phys. Lett. **89**, 171911 (2006).
[20] F. Ye, T. Mori, D. R. Ou, J. Zou, and J. Drennan, J. Nanosci. Nanotechnol. **7**, 2521 (2007).
[21] R. F. Egerton, *Electron Energy-Loss Spectroscopy in the Electron Microscope* (Plenum Press, New York, 1986).
[22] G. Kaindl, G. Kalkowski, W. D. Brewer, B. Perscheid, and F. Holtzberg, J. Appl. Phys. **55**, 1910 (1984).
[23] B. T. Thole, G. van der Laan, J. C. Fuggle, G. A. Sawatzky, R. C. Karnatak, and J.-M. Esteva, Phys. Rev. B **32**, 5107 (1985).
[24] T. Manoubi and C. Colliex, J. Electron Spectrosc. Relat. Phenom. **50**, 1 (1990).
[25] S. Arai, S. Muto, J. Murai, T. Sasaki, Y. Ukyo, K. Kuroda, and H. Saka, Mater. Trans. **45**, 2951 (2004).
[26] L. A. J. Garvie and P. R. Buseck, J. Phys. Chem. Solids **60**, 1943 (1999).
[27] N. V. Skorodumova, S. I. Simak, B. I. Lundpvist, I. A. Abrikosov, and B. Johansson, Phys. Rev. Lett. **89**, 166601 (2002).
[28] H. Hayashi, R. Sagawa, H. Inaba, and K. Kawamura, Solid State Ionics **131**, 281 (2000).
[29] A. Travlos, N. Boukos, G. Apostolopoulos, and A. Dimoulas, Appl. Phys. Lett. **82**, 4053 (2003).
[30] A. V. Soldatov, T. S. Ivanchenko, S. Della Longa, A. Kotani, Y. Iwamoto, and A. Bianconi, Phys. Rev. B **50**, 5074 (1994).
[31] L. Douillard, M. Gautier, N. Thromat, M. Henriot, M. J. Guitter, J. P. Duraud, and G. Tourillon, Phys. Rev. B **49**, 16171 (1994).
[32] P. Li, I. W. Chen, J. E. Penner-Hahn, and T. Y. Tien, J. Am. Ceram. Soc. **74**, 958 (1991).
[33] H. Nitani, T. Nakagawa, M. Yamanouchi, T. Osuki, M. Yuya, and T. A. Yamamoto, Mater. Lett. **58**, 2076 (2004).